Dissociative multiphoton ionization of NO_2 studied by time-resolved imaging

André T. J. B. Eppink and Benjamin J. Whitaker[a)]
School of Chemistry, University of Leeds, Leeds LS2 9JT, United Kingdom

Eric Gloaguen and Benoit Soep
Laboratoire Francis Perrin, CEA/DRECAM Service des Photons, Atomes et Molécules, C.E.N. Saclay, 91191 Gif-sur-Yvette Cedex, France

A. Marcela Coroiu and David H. Parker
Department of Laser Physics, University of Nijmegen, 6500 GL Nijmegen, The Netherlands

(Received 22 March 2004; accepted 29 July 2004)

We have studied dissociative multiphoton ionization of NO_2 by time-resolved velocity map imaging in a two-color pump-probe experiment using the 400 and 266 nm harmonics of a regeneratively amplified titanium-sapphire laser. We observe that most of the ion signal appears as NO^+ with ~0.28 eV peak kinetic energy. Approximately 600 fs period oscillations indicative of wave packet motion are also observed in the NO^+ decay. We attribute the signal to two competitive mechanisms. The first involving three-photon 400 nm absorption followed by dissociative ionization of the pumped state by a subsequent 266 nm photon. The second involving one-photon 400 nm absorption to the $^2B_2$ state of NO_2 followed by two-photon dissociative ionization at 266 nm. This interpretation is derived from the observation that the total NO^+ ion signal exhibits biexponential decay, $0.72\exp(-t/90\pm10)+0.28\exp(-t/4000\pm400)$, where t is the 266 nm delay in femtoseconds. The fast decay of the majority of the NO^+ signal suggests a direct dissociation via the bending mode of the pumped state. © *2004 American Institute of Physics.*
[DOI: 10.1063/1.1795654]

I. INTRODUCTION

Femtosecond time-resolved imaging spectroscopy is emerging as a practical and versatile technique with which to study nonadiabatic processes in polyatomic molecules.[1] The time-resolved photoelectron kinetic energy spectrum[2] and its concomitant angular distribution[3] are sensitive probes of internal conversion,[4] vibrationally mediated spin-orbit coupling (intersystem crossing),[5] intracluster reaction dynamics,[6,7] dissociative ionization,[8] reaction mechanism,[9] and other non Born-Oppenheimer dynamics.[10] Measurements of the time evolution of the photoion signal are in general less sensitive to the details of the electronic dynamics because the photoionization cross section is not so affected by vibronic coupling as the energy of the ejected electron, but nonetheless important information can be gleaned from such measurements.[11]

For many years, NO_2 has served as a benchmark polyatomic molecule for studies into unimolecular reaction dynamics, intramolecular vibrational redistribution, and vibronic coupling because of its rich and complex behavior despite its apparent simplicity as a triatomic molecule. There is an extensive literature, too vast to review here, concerning frequency domain studies of the dynamics of NO_2. Developments in short pulse lasers have also prompted a number of groups to revisit the dynamics of this intriguing molecule in the time domain in recent years. In particular, Wittig and co-workers[12–14] and Troë and co-workers[15,16] have measured the energy dependence of the unimolecular rate coefficients close to the dissociation threshold. These measurements are a sensitive test of statistical theories which predict a microcanonical unimolecular rate constant given by

$$k(E)=\frac{N^{\ddagger}(E-E_0)}{h\rho(E)}, \tag{1.1}$$

where E_0 is the reaction threshold, $N^{\ddagger}(E-E_0)$ is the number of open channels at the transition state, and $\rho(E)$ is the density of coupled molecular states at the energy E.

Of course, time resolution comes at the expense of energy resolution. Wittig and co-workers employed pump-probe photofragment excitation (PHOFEX) spectroscopy, in which they monitored the appearance of the NO product by laser induced fluorescence (LIF). Close to threshold the temporal resolution of a picosecond (10–25 ps) experiment is adequate to resolve the dissociation rate, 0.02×10^{12} s^{-1}, whilst at the same time giving reasonable energy resolution (~2–3 cm^{-1}) but by 25 cm^{-1} of excess energy the rate rises to over 0.13×10^{12} s^{-1} which is at the limit of the resolution of a 10 ps pulse. In other experiments using a femtosecond laser Ionov *et al.*[12] were able to measure $k(E)$ up to about 800 cm^{-1} of excess energy where the rate is 1.3×10^{12} s^{-1} but at the cost of energy resolution (40–70 cm^{-1}). Troë and co-workers adopted a slightly different approach and observed the depletion of the dissociating NO_2 by monitoring the LIF signal from the $1\,^2\Pi_g(3d)$ and $1\,^2\Sigma_u^+(3p)$ Rydberg

a)Author to whom correspondence should be addressed. Electronic mail: b.j.whitaker@chemistry.leeds.ac.uk

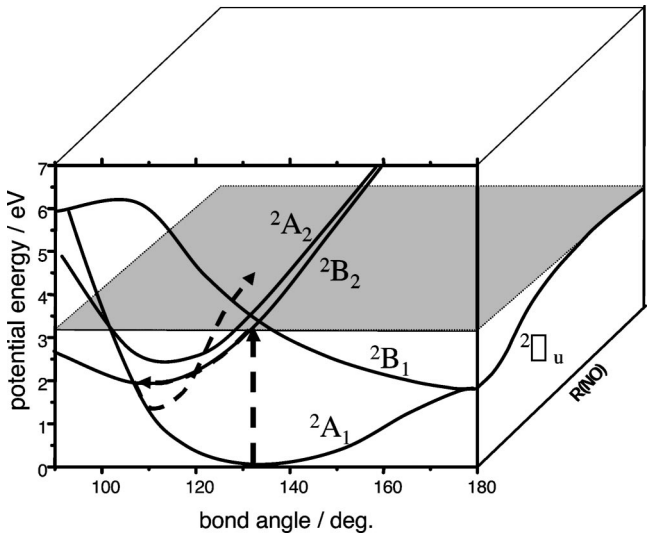

FIG. 1. The four lowest lying electronic states of NO_2 are strongly coupled by vibronic interactions. The pairs of states labeled $^2A_1$, $^2B_1$, and $^2A_2$, $^2B_2$ are components of a Renner-Teller pair correlating to $^2\Pi_u$ and $^2\Gamma_g$ states in linear geometry. In the near UV the dominant absorption occurs for transitions from the $^2A_1$ ground state to the $^2B_2$ state. For wavelengths below 397.9 nm this leads to dissociation on the ground state surface via the path indicated in the figure in which the excited molecule initially relaxes towards the minimum of the $^2B_2$ state, inducing motion that tightens the bond angle. At a bond angle of about 114° the $^2B_2$ adiabat crosses through the ground state. Close to this point the Born-Oppenheimer approximation is not valid and the electronic character of the excited state is mixed with that of the ground state. A wave packet created by a short pump pulse can then cross to the $^2A_1$ state where it continues to evolve along the O-NO stretching coordinate, eventually leading to dissociation into $NO(X\,^2\Pi)$ and $O(^3P)$.

states in a femtosecond pump-probe experiment. By varying the temperature of the sample but keeping the photolysis wavelength fixed the effect of rotational excitation on the decay rate, $k(E,J)$, was also measured in these experiments. The results of both the Wittig and Troë groups are in broad agreement and both are consistent with the predictions from statistical unimolecular rate theory. However, structure is apparent in the detailed energy dependence of $k(E,J)$ and on a microscopic level the dissociation appears to be governed by specific resonance states whose widths show fluctuations around average values which are related to the specific rate constants from statistical theories.[17]

The complexity observed in the detailed energy dependence of the unimolecular rate constants is also manifest in the near UV absorption spectrum of NO_2 both above and below the first dissociation threshold[18] of 25 128.57 $\pm 0.05\ cm^{-1}$ and is due to the vibronic coupling between the four lowest electronic states of molecule (see Fig. 1). Around this excitation energy the absorption cross section is dominated by transitions from the $\tilde{X}\,^2A_1$ ground state to the $\tilde{A}\,^2B_2$ state with little contribution to the $\tilde{B}\,^2B_1$, $\tilde{C}\,^2A_2$ states. However, the $\tilde{A}\,^2B_2$ state is embedded within the $\tilde{X}\,^2A_1$ electronic ground state and is strongly coupled to it due to a conical intersection between the two potential energy surfaces (PESs). Excitation above the conical intersection therefore leads to rapid internal conversion and an extremely complicated absorption spectrum.[19] Above the dissociation limit to $NO(^2\Pi)+O(^3P)$ on the $\tilde{X}\,^2A_1$ surface the situation leads to equally rich dynamics, manifest, for example, in the observation of "Ericson fluctuations" [20] in the PHOFEX spectra[21] and in the photofragment aniostropy parameter.[22]

The nuclear dynamics leading to dissociation is now generally agreed to involve a decrease in bending angle as the molecule moves from the Franck-Condon region of the $\tilde{A}\,^2B_2$ state immediately accessed by the photolysis photon towards the conical intersection with the $\tilde{X}\,^2A_1$ state. Once the electronic character reverts to the $\tilde{X}\,^2A_1$ state the nuclear dynamics follow a stretching motion along the O-NO coordinate. Support for this model comes from *ab initio* calculations. One such recent calculation[23] locates the $\tilde{X}\,^2A_1/\tilde{A}\,^2B_2$ conical intersection at $R=131.1$ pm and $\alpha=113.6°$ at an energy $T_e=1.210$ eV above the ground state minimum ($R=118.7$ pm and $\alpha=133.8°$).[24] This model is also supported by observations of the NO product state and angular distributions as observed by ion imaging[25] or velocity mapping,[26] for example, and in the time domain by the elegant photoelectron-photoion coincidence imaging experiments of Davies *et al.*[27,28]

Importantly for the discussion that follows, the experiments of Davies *et al.*, which were carried out at a single wavelength of 375 nm for both pump and probe pulses (width 100 fs, intensity $\sim 10^{12}\ W\,cm^{-2}$), identified a dissociative multiphoton ionization (DMI) pathway due to a three-photon excitation of NO_2 to a repulsive potential correlating with $NO(C\,^2\Pi)+O(^3P)$ followed by single-photon ionization of NO to form $^1\Sigma^+$ ground state NO^+. This finding was not in accord with earlier work of Singhal *et al.*[29] who had investigated the multiphoton ionization and dissociation pathways of NO_2 in a single pulse. These experiments also employed 375 nm light but with shorter 50 fs pulses and an estimated intensity of up to $5\times10^{13}\ W\,cm^{-2}$, and had concluded that the observed NO^+ signal was due to one-photon excitation of the $\tilde{A}\,^2B_2$ state of NO_2 followed by electronic predissociation on the ground state PES and subsequent three-photon ionization of $NO(X\,^2\Pi)$. Some signal from N^+ and O^+ was also observed and attributed to dissociation of the NO molecule.

In order to investigate the effects of laser field intensity on the multiphoton dissociation dynamics of NO_2 in more detail López-Martens, Schmidt, and Roberts[30] employed two-color fluorescence depletion spectroscopy using a 400 nm pump and 800 nm probe. Dissociative production of NO in the $A\,^2\Sigma^+$ state was monitored through the depletion of the $A\,^2\Sigma^+\rightarrow X\,^2\Pi$ fluorescence induced by the 800 nm probe. For 400 nm pump intensities between $\sim 3\times10^{12}$ and $2\times10^{13}\ W\,cm^{-2}$ these authors concluded that the dominant dissociation pathway involved three-photon absorption of 400 nm light to a highly excited state of NO_2 (situated ~9.3 eV above the ground state minimum). This state was estimated to dissociate to $NO(A\,^2\Sigma^+, v=0,1,\text{ and } 2)+O(^3P)$ on a time scale no longer than 600 fs. Thus the primary dissociation mechanism is similar to that proposed by Davies *et al.*[27] although a different intermediate electronic state of NO_2 must be involved since three-photon 400 nm excitation has insufficient energy to reach the $NO(C\,^2\Pi)+O(^3P)$ as-

ymptote even in a room temperature sample of NO_2.

In this paper we report our first attempts to follow the dynamics of the internal conversion and the subsequent dissociation of an optically prepared sample of NO_2 in the $\tilde{A}\,^2B_2$ state as it crosses over to the ground $\tilde{X}\,^2A_1$ state by time-resolved imaging of both photoelectrons and photoions. The thesis of our experiment is that as the electronic configuration changes from $[\cdots](5a_1)^2(1a_2)^2(4b_2)^1(6a_1)^2$ to $[\cdots](5a_1)^2(1a_2)^2(4b_2)^2(6a_1)^1$ we expect to be able to detect a change in the photoelectron kinetic energy release spectrum (and its angular distribution). Concomitant changes are also to be expected in the time-resolved photoion yield spectrum as the nuclear dynamics cause the molecule to sample different Franck-Condon windows to the cation.

The paper is organized as follows: in Sec. II we describe specific features of the Saclay Laser-Matter Interactions Center (SLIC) laser facility and the general experimental arrangement. Section III describes the observations. The key observations are a sub 100 fs rise time followed by a longer lived oscillatory decay in the NO^+ signal as a function of the 266 nm delay, and that the NO^+ ions are observed with significant translational energy. These results are interpreted in Sec. IV in terms of a DMI mechanism that is similar to that previously proposed by López-Martens *et al.*,[30] but which may also be sensitive to the internal conversion dynamics between the $\tilde{X}\,^2A_1/\tilde{A}\,^2B_2$ states of NO_2. Finally we draw together our conclusions in Sec. V.

II. EXPERIMENT

The experimental apparatus used for the real time experiments reported here associates a pulsed supersonic beam with an ion/electron imaging device. It is coupled to the SLIC femtosecond laser facility. The master laser is a titanium-sapphire regenerative amplifier centered at 800 nm and operated at 20 Hz repetition rate. For our experiments, the pump and probe pulses at 400 and 266 nm, respectively, are generated by frequency mixing. The 800 nm output is split into two beams after recompression, yielding a 40 fs pulse (full width at half maximum). Beam splitting is accomplished by a tilted window, the coupling being polarization sensitive. Thus the intensity ratio between both pump and probe beams can be varied continuously by the rotation of a half wave plate. The pump beam is used directly after frequency doubling whilst the other beam is delayed before third harmonic generation, by an optical delay line. The two beams, pump and probe, are recombined in the vacuum chamber at a small angle and independently focused onto the molecular beam by thin lenses outside the chamber. The cross correlation width of the laser pulses is of the order of 90 fs as measured by nonresonant three-photon ionization of NO diluted in He. The pulse energies that are injected into the machine are up to 100 μJ at 400 nm and 70 μJ at 266 nm, but typically 10–15 μJ at 400 nm and 5–15 μJ at 266 were used. They are focused to a 200 μm diameter spot yielding a typical intensity of 5×10^{11} W cm^{-2}. The pump and probe beam polarization are generally set parallel and they are also parallel to the imaging plane.

The supersonic beam has already been described in a previous paper.[31] For the current experiments a 2% NO_2/5% O_2/helium gas mixture was expanded through a pulsed nozzle, 300 μm in diameter. O_2 was added to the gas mixture in order to displace the NO_2/NO equilibrium towards NO_2. The backing pressure was maintained at a relatively low value of 1.2 bar in order to minimize the production of N_2O_4 and higher clusters. However, from the known equilibrium constant (0.15) for $N_2O_4 \rightleftharpoons 2NO_2$ at 25 °C the N_2O_4 concentration still comprises 50% of the sample. This does not affect measurements with the 400 nm pump since the absorption of NO_2 dominates at this wavelength. The opposite is true at 266 nm where N_2O_4 absorbs weakly, while NO_2 is transparent.

A velocity map ion/electron imaging device based on the design of Eppink and Parker[32] has been used. The electrostatic optics are arranged in our apparatus to image perpendicular to the molecular beam. This configuration does not give the best resolution for the angular distributions of the ion images[33] owing to the velocity spread in the supersonic beam, however, the major contribution to the spread in velocity distributions arises from the femtosecond excitation with ca. 40 meV width. Perpendicular extraction has the advantage of allowing easy visualization of the molecular beam translational cooling and hence its optimization. The perpendicular configuration has also been chosen to allow a Wiley-McLaren time-of-flight mass (TOF) spectrometer to be placed opposite the imager. The TOF allows convenient optimization of the pump-probe conditions and survey spectra of the various photoions.

Since the electric fields in a velocity map imaging spectrometer can be adjusted to magnify the velocity map to practically any size, the pixel-to-velocity calibration factor for any given set of focusing voltages of the spectrometer needs to be measured.[34] For this purpose, we use photoelectron images from xenon at 10^{-6} Torr obtained by three-photon 266 nm ionization. This results in $Xe^+\,^2P_{3/2}$ and $^2P_{1/2}$ ions with an energy separation of 1.31 eV.

The images from the microchannel plate (MCP)/phosphor detector are collected in time step multiples of 0.67 fs using a charge-coupled device camera (LaVision), in which mass resolution is achieved by gating the voltage applied to the MCPs. The images are stored and processed (e.g., averaged) using the DAVIS software package (LaVision) at each delay step. Each raw image is then inverted by the Hankel method or by simulation using a sum of Gaussians.[35]

III. RESULTS

The pump-probe scheme of the present experiments is illustrated in Fig. 2. The pump pulse, centered at ~400 nm, excites jet-cooled molecules initially in the lowest vibrational and rotational levels of the $\tilde{X}\,^2A_1$ state to zero-order rovibrational levels of the $\tilde{A}\,^2B_2$ state. The population in the $\tilde{A}\,^2B_2$ state can be probed by two-photon ionization through a number of Rydberg states [$1\,^2\Sigma_u^+(3p)$ is illustrated] converging to the $X\,^1\Sigma_g^+$ state of NO_2^+ or as in the experiments of Abel *et al.*[36] by monitoring the fluorescence from these

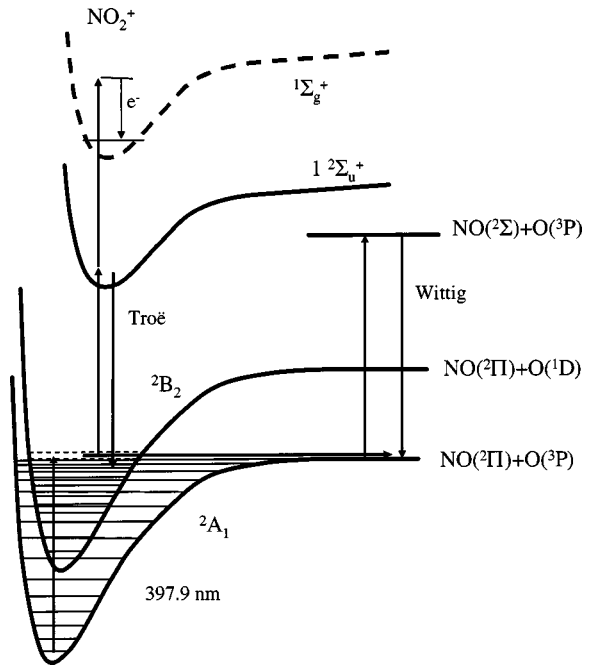

FIG. 2. The pump-probe schemes adopted by Troe and co-workers (Ref. 36) and Wittig and co-workers (Ref. 42) are illustrated together with our proposed ionization scheme. The pump pulse in all the schemes is chosen close to 400 nm in order to excite the $\tilde{A}\,^2B_2$ state close to the dissociation limit on the $\tilde{X}\,^2A_1$ state. As the result of internal conversion, the electronic character of the optically prepared state evolves in time. This can be detected by following the evolution of the photoelectron spectrum.

intermediate states. In our experiments, we detect NO^+, NO_2^+ and photoelectrons as a function of the pump-probe delay.

Because of the linear momentum conservation of the nuclei upon ionization, the relatively low lying zero-order vibrational levels of the $\tilde{A}\,^2B_2$ state will preferentially prepare equally low lying vibrational levels of the ground electronic state of the cation ($^1\Sigma_g^+$) with near maximal available kinetic energy to the photoelectron, whereas the reverse will be true for the relatively high lying vibrational states of the $\tilde{X}\,^2A_1$ state, the time evolution of the photoelectron kinetic energy release (KER) spectrum thus provides a potentially sensitive probe of the internal conversion dynamics. The difficulty in the case of NO_2 is that the ground state of the cation and the Rydberg ''stepping stone'' states are all linear whereas the conical intersection between the $\tilde{X}\,^2A_1/\tilde{A}\,^2B_2$ valence states occurs around $\alpha = 114°$ so the ionization cross section is expected to vary considerably with bending angle.

Figures 3 and 4 show the total ion signals, integrated over all recoil speeds, measured for NO^+ and NO_2^+, respectively, as a function of the pump (400 nm)-probe (266 nm) delay. The insets show the velocity map ion images for the two species at zero time delay. The striking observation of kinetic energy release in the NO^+ signal at time zero immediately suggests that the ionization scheme is more complex than that just outlined, and is one of the main results of this study that needs to be explained. When examined in more detail, Fig. 5, the NO^+ signals also exhibit structure indicative of wave packet motion. The data shown in the figure

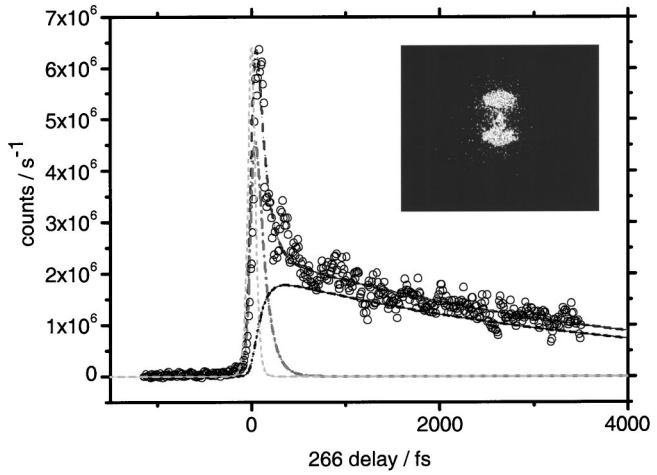

FIG. 3. The total NO^+ ion signal recorded as a function of the delay of a probe pulse centered at 266 nm following excitation of NO_2 around 400 nm. The energies of the pump and probe pulses were 15 and 5 μJ, respectively. The decay of the NO^+ transient can be fit by forward convolution with a 90 fs laser pulse to a biexponential function with time constants of 90 ± 10 and 4000 ± 400 fs and weightings of 72% and 28%, respectively, as shown by the solid line in the figure. The inset shows the velocity map ion image recorded at the peak of the transient.

come from three experimental runs taken at different temporal resolution recorded over 2 days. Each experimental run consisted of between 10 and 12 sequences. Each sequence measured the total ion count for the average of four ion images taken at each time step. The points represent the average signal over the whole sequence, and the error bar one standard deviation. Although the oscillations in the total ion signal are small, the statistics are convincing.

IV. DISCUSSION

Nitrogen dioxide is unusual in that more NO^+ ions are produced than NO_2^+ at low excitation energy, both by electron-impact ionization and by photoionization, which is

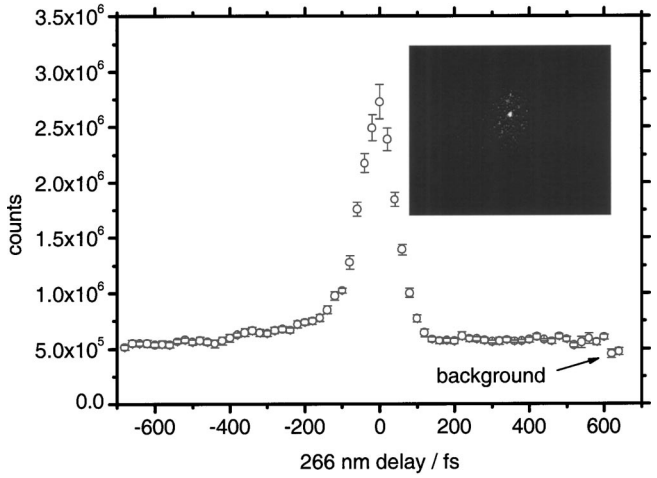

FIG. 4. The total NO_2^+ ion signal recorded as a function of the delay of a probe pulse centered at 266 nm following excitation of NO_2 around 400 nm. The energies of the pump and probe pulses were 15 and 5 μJ, respectively. The points labeled background were recorded at a time delay of 10 ps. The inset shows the velocity map ion image recorded at the peak of the transient.

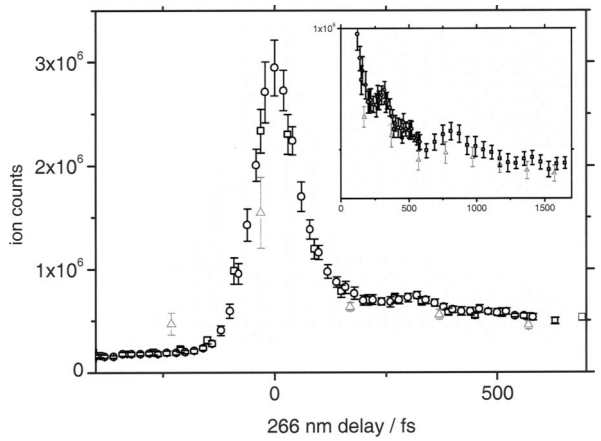

FIG. 5. The NO^+ ion signal recorded as a function of the delay of a probe pulse centered at 266 nm following excitation of NO_2 around 400 nm at higher temporal resolution than Fig. 4. Each point in the figure represents the average of between 10 and 12 independent scans. The different symbols (circles, squares, and triangles) indicate data taken on different experimental runs. Operating conditions were kept as close as possible between one run and another but inevitably there are small differences in the average pulse energy, etc., between runs. The error bars represent one standard deviation. The inset shows an expansion of part of the decay.

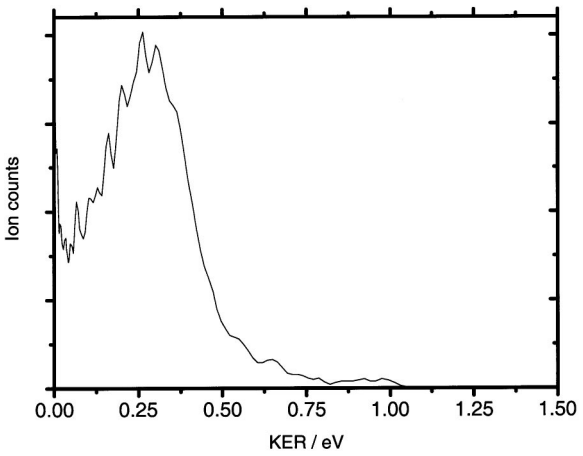

FIG. 6. Kinetic energy release (KER) spectrum of NO^+ following dissociative multiphoton ionization of NO_2 by 400 and 266 nm light. The spectrum shown is obtained by Abel inversion of the velocity map image of the ion recorded at zero delay between the two pulses as described in the text.

explained by the fact that the neutral is bent while the ion is linear.[37] There was consequently uncertainty as to the ionization potential (IP) of the molecule in the early literature. The NIST Chemistry WebBook database[38] gives the evaluated adiabatic IP as 9.586 ± 0.002 eV. This rather precise value was obtained by Haber *et al.*[39] in an elegant three-color experiment in which two-photon excitation was used to excite the bent molecule to a linear Rydberg state from which a third photon could be used to ionize the molecule without the Franck-Condon constraints encountered in direct photoionization or electron-impact measurements with values ranging from 10.4 to 11.23 eV.

Davies *et al.* have studied the time-resolved photoelectron angular distributions during the photodissociation of NO_2 in a one-color pump-probe experiment at 375.3 nm.[28] Their data can be interpreted as being due to three-photon excitation to an unspecified electronic state of NO_2 which dissociates to $NO(C\,^2\Pi) + O(^3P)$. A fourth photon later ionizes $NO(C\,^2\Pi)$ whereafter the photoelectrons and photoions can be imaged in coincidence. The two-color experiments of López-Martens *et al.*[30] using a 400 nm pump and 800 nm probe can be interpreted in terms of a similar mechanism but now with the pumped state of NO_2 dissociating to $NO(A\,^2\Sigma^+) + O(^3P)$. The initially excited electronic state of NO_2 cannot be the same in the two mechanisms since three photons of 400 nm do not have enough energy to reach the C state of NO, 9.579 eV above the ground state of NO_2.

In our experiments, a prompt NO^+ signal is observed as a function of the 266 nm delay (Fig. 3). The best fit rise time of the signal is ~57 fs (although since this is of the same order as the cross-correlation time of the two pulses all we can say is that the rise time is on the same time scale as the excitation). The kinetic energy of the NO^+ fragment can be obtained by Abel inversion of the ion image shown in the inset to Fig. 3. The ion KER spectrum is shown in Fig. 6. It is quite broad and unstructured and peaks about 280 meV.

If we assume three-photon excitation at 400 nm to a state that dissociates to $NO(A\,^2\Sigma^+, v=0)$ plus $O(^3P)$ according to the mechanism proposed by López-Martens *et al.* then the maximum expected KER into the NO dissociation product would be 0.166 eV (the total excess energy, including the zero-point vibrational energy in the NO moiety, for this channel is 0.585 eV). One could imagine similar photofragmentation pathways to the NO $B\,^2\Pi$ state or, possibly, the $a\,^4\Pi$ state, where the maximum KER in the zeroth vibrational state of the NO channel would be 0.121 eV or 0.421 eV, respectively. However, none of these pathways agrees with the observed KER, and furthermore the $a\,^4\Pi$ channel is spin forbidden. The immediate absorption of a fourth 266 nm photon from the intermediate state is capable of producing a NO^+ fragment with sufficient excess energy to agree with the observations. The excess energy for the process

$$NO_2 \xrightarrow{3\times 400\ \text{nm}} NO_2^{**} \xrightarrow{266\ \text{nm}} NO^+(^1\Sigma^+, \nu=0) + O(^3P) \tag{4.1}$$

is 0.85 eV, which would result in an ionic fragment with up to 0.21 eV of kinetic energy. The discrepancy between this value and the observed KER of 0.28 eV can easily be explained by the considerable energy spread of the four photons, but a difficulty with this interpretation is its oscillatory decay (Fig. 5).

López-Martens *et al.*[30] observe a rise time of order 600 fs for the $NO(A\,^2\Sigma^+)$ signal. This is similar to the 350–500 fs time scale for O-NO bond cleavage observed by Davies and company.[27] These times are more consistent with an indirect dissociation mechanism involving electronic predissociation similar to that observed for the $\tilde{A}\,^2B_2/\tilde{X}\,^2A_1$ states. The prompt appearance of the NO^+ signal we observe is more consistent with a direct dissociation involving a bending mode of the molecule, where the vibrational frequency varies from 560 cm^{-1} in the $\tilde{H}$ state to 750 cm^{-1} in the $\tilde{X}$ state and is possibly as fast as 896 cm^{-1} in the $\tilde{B}$ state.[40]

A rapid buildup time has also been observed by Assenmacher *et al.*[41] in the NO^+ transient observed in the photo-

dissociation dynamics of HNO_3 following 200 nm excitation of the S_3 state. This signal was unambiguously assigned to ionization of the primary photodissociation product NO_2 by three photons of the 400 nm probe. Although there is some uncertainty as to the electronic state of the NO_2 photofragments, the $S_3\ 2\,^1A'$ state of HNO_3 correlates with the $\tilde{A}\,^2B_2$ state of NO_2 and it seems highly probable that Assenmacher *et al.* observed three-photon ionization of the $\tilde{A}\,^2B_2$ state via the dissociative ionization channel. Since three photons of 400 nm light are energetically equivalent to two of 266 nm, we could be observing the process:

$$\mathrm{NO_2}(\tilde{X}\,^2A_1) \xrightarrow{400\ \mathrm{nm}} \mathrm{NO_2}(\tilde{A}\,^2B_2),$$

$$\mathrm{NO_2}(\tilde{A}\,^2B_2) \xrightarrow{2\times 266\ \mathrm{nm}} \mathrm{NO_2^{**}} \rightarrow \mathrm{NO^+}(^1\Sigma^+) + \mathrm{O}(^3P) + 0.043\mathrm{eV}. \quad (4.2)$$

The buildup time of the NO^+ signal that we observe is consistent with that observed by Assenmacher *et al.* (80 ± 20 fs), but the mechanism is inconsistent with the observation of KER in the NO^+ fragment.

When we examine the decay of the total NO^+ signal (Fig. 3) we find that the data can be fit by the biexponential function $0.72\exp(-t/90\pm 10) + 0.28\exp(-t/4000\pm 400)$ with t in fs (266 nm delay), which suggests that we are observing competing processes. The faster component is probably due to a three-photon excitation at 400 nm to a state that dissociatively ionizes on the absorption of a fourth 266 nm photon (process 4.1). From the rapid rise time of the signal we conclude that the reaction coordinate for this channel is barrierless and via a bending mode. The slower component, which is only observable for slow NO^+ ions, may be due to the alternative DMI scheme involving one-photon absorption of 400 nm light of the $\tilde{A}\,^2B_2$ state followed by two-photon 266 nm excitation to another highly excited state of NO_2 which auto ionizes to $\mathrm{NO^+}(^1\Sigma^+) + \mathrm{O}(^3P)$ (process 4.2).

If this interpretation were correct, we would expect the NO^+ signal at long times to decay on a time scale consistent with the internal conversion rate of NO_2 $\tilde{A}\,^2B_2$ to $\tilde{X}\,^2A_1$. This is indeed the case. For long 266 nm delays a decay time of 4000 ± 400 fs is entirely consistent with the previous observations of Ionov *et al.*[12,42] and of Abel *et al.*[15] bearing in mind that the 400 nm pump laser in our experiments is broad and excites zero-order levels in the NO_2 $\tilde{A}\,^2B_2$ state both above and below the dissociation limit on the $\tilde{X}\,^2A_1$ state PES.

Interestingly when examined at higher resolution the decay of the NO^+ signal exhibits oscillations (Fig. 5). The Fourier transform of the decay trace reveals a dominant contribution to the oscillations with a period of about 600 fs corresponding to an energy level spacing of 55 cm^{-1}. If our interpretation of the origin of the NO^+ transient is correct, this is the first direct measurement of the energy level density of the coupled levels in the mixed $\tilde{X}\,^2A_1/\tilde{A}\,^2B_2$ state of NO_2 close to the conical intersection. The resonance structure close to the threshold has recently been calculated by Abel *et al.*[17] and has been proposed as the explanation for the step structure observed in the energy dependence of the unimolecular rate constants by Wittig and co-workers.[12,14,42] Our observation of an average energy level spacing of 55 cm^{-1} is consistent with this emerging picture of the dissociation dynamics. However, other explanations for the wave packet motion cannot be ruled out. For example, despite our contention that the dissociation of the initially pumped electronic state of NO_2 in process 1.2 is direct, we might be observing competition with an electronic predissociation via a conical intersection similar to that known to occur between the ground and first excited electronic states.

Finally, we turn to the interpretation of the NO_2^+ data shown in Fig. 4. The inset shows the ion image obtained at time zero. There is some evidence of a N_2O_4 or cluster contribution to the signal since some ions are observed with kinetic energy, but this is a small contribution to the total signal. We have, however, already observed that the photoionization of NO_2 is unusual in that close to threshold more NO^+ is observed than NO_2^+ because of the geometry change upon ionization and the linear nature of the Rydberg states. As mentioned in Sec. II, NO_2 does not absorb light at 266 nm, therefore the long lived signal at negative 266 nm delays, i.e., 266 nm pumping, pertains to N_2O_4 and corresponds to ionization by three 400 nm photons. This accounts for the weak signal and the dissociation of N_2O_4: the IP of N_2O_4 is 10.8 ± 0.2 eV, although the vertical value is higher at around 11.5 eV, and one photon of 266 nm light plus two of 400 nm yields 10.8 eV. Thus the absorption of a further photon of 400 nm light will provide more than enough energy to dissociate $N_2O_4^+$ to form energetic NO_2^+.

The majority of the NO_2^+ ions have zero kinetic energy as expected for a signal from the monomer. We cannot attribute the majority of the observed NO_2^+ signal to a mechanism involving one photon 400 nm pumping of the $^2B_2$ state followed by two-photon ionization via the $1\,^2\Pi_g(3d)$ and $1\,^2\Sigma_g^+(3p)$ Rydberg states, because the decay (54 ± 40 fs) of the signal for long 266 nm delay is far faster than the decay of the UV fluorescence measured by Abel *et al.*[15] However the decay of the NO_2^+ signal is comparable to the rise time of the NO^+ signal we measure. This observation fits with our proposed NO^+ production mechanism and suggests that most of the NO_2 population is lost through a dissociative ionization route, such as (4.1), rather than by internal conversion to the $\tilde{X}\,^2A_1$ state followed by dissociation. There is, however, a noticeable plateau to the long time decay of the NO_2^+ signal that persists for several picoseconds. This is most likely due to NO_2 $\tilde{A}\,^2B_2$ molecules pumped to levels below the dissociation threshold. However, our signal-to-noise ratio is not yet good enough to detect recurrences in this signal which would be expected as population oscillates between the coupled electronic states. The growth in the NO_2^+ signal is consistent with 400 nm pumping of the NO_2 $\tilde{A}\,^2B_2$ state followed by two-photon ionization, but the interpretation is clouded by the potential interference from the presence of N_2O_4 in the sample.

V. CONCLUSIONS

We have studied dissociative multiphoton ionization (DMI) of NO_2 by time-resolved velocity map imaging in a

two-color pump-probe experiment using the 400 and 266 nm harmonics of Saclay femtosecond laser facility (SLIC). We observe that most of the ion signals appear as NO^+ following DMI. As a function of 266 nm delay, the total NO^+ ion signals exhibit biexponential decay.

$$0.72\exp(-t/90\pm 10)+0.28\exp(-t/4000\pm 400)$$

with t in fs, and ~600 fs period oscillations due to wave packet motion are also observed.

Close to the cross correlation of the two pulses the NO^+ ions are observed to have ~280 meV peak kinetic energy. This value is consistent with, but not exactly in accord with, the three-photon dissociation mechanism

$$NO_2 \xrightarrow{3\times 400\ \text{nm}} NO(A\,^2\Sigma^+)+O(^3P)$$

which has previously been proposed by López-Martens *et al.*[30] These earlier investigations had observed the process by pump-probe depletion spectroscopy of the NO $A\,^2\Sigma^+$ state with a subsequent 800 nm pulse. In our experiments the resulting NO $A\,^2\Sigma^+$ molecules could be ionized by a subsequent 266 nm pulse, but with only ~167 meV of kinetic energy in the $v=0$ channel. Our observation of a rapid rise time to the NO^+ signal coupled with the 280 meV kinetic energy release suggests that a different mechanism is operating in which a component of the photoions arises from a dissociative multiphoton ionization channel involving the absorption of a fourth 266 nm photon from the bending mode of the pumped state when the NO moiety is still essentially bound to the O atom.

Some NO^+ signal is also observed with low kinetic energy release. These ions could be produced by the alternative mechanism

$$NO_2(\tilde{X}\,^2A_1) \xrightarrow{400\ \text{nm}} NO_2(\tilde{A}\,^2B_2) \xrightarrow{2\times 266\ \text{nm}} NO_2^{**}\rightarrow NO^+(^1\Sigma^+)+O(^3P)+e^-$$

with a total excess energy of 43 meV. Some support for the possibility of this channel comes from our observation of a small number of NO_2^+ ions at very long 266 nm delays which suggests that at least some NO_2 ($\tilde{A}\,^2B_2$) population is created in our experiments.

Oscillations indicative of wave packet motion are observed in the NO^+ decay. These may measure the average energy level spacing between the resonant levels of the $\tilde{A}\,^2B_2/\tilde{X}\,^2A_1$ states close to their conical intersection, but alternative explanations cannot be ruled out. For example, although our data suggest that the intermediate state pumped by three photons of 400 nm light dissociates directly it is possible that there is competition with an indirect route to $NO(A\,^2\Sigma^+)+O(^3P)$. Such a mechanism would be consistent with the observations of López-Martens *et al.*,[30] who observed an approximately 600 fs rise time in the $NO(A\,^2\Sigma^+)$ signal.

Further work is ongoing in our laboratories to improve the energy resolution of the photoelectron imaging spectrometer used in these experiments. This will allow us to characterize better the intermediate states involved in the DMI process.

ACKNOWLEDGMENTS

The authors are grateful to Shaijal Patel for assistance in the data processing of the NO^+ kinetic energy release spectrum. A.T.J.B.E. is grateful to the European Union for a postdoctoral fellowship funded through the PICNIC HPRN-CT-2002-00183 network. B.J.W. and D.H.P. are also grateful to the European Union for support to access the SLIC/LASERNET ultrafast laser facility at CEA, Saclay. D.H.P. and A.M.C. thank the Dutch National Science Foundation NWO-CW and the van Gogh program VG-66-136 for support.

[1] A. V. Davis, R. Wester, A. E. Bragg, and D. M. Neumark, J. Chem. Phys. **118**, 999 (2003); T. Suzuki and B. J. Whitaker, Int. Rev. Phys. Chem. **20**, 313 (2001).
[2] A. Stolow, Annu. Rev. Phys. Chem. **54**, 89 (2003).
[3] T. Seideman, Annu. Rev. Phys. Chem. **53**, 41 (2002); K. L. Reid, *ibid.* **54**, 397 (2003).
[4] B. Soep, J. M. Mestdagh, S. Sorgues, and J. P. Visticot, Eur. Phys. J. D **14**, 191 (2001).
[5] M. Tsubouchi, B. J. Whitaker, L. Wang, H. Kohguchi, and T. Suzuki, Phys. Rev. Lett. **86**, 4500 (2001).
[6] M. Tsubouchi, C. A. de Lange, and T. Suzuki, J. Chem. Phys. **119**, 11728 (2003).
[7] J. M. Mestdagh, B. Soep, M. A. Gaveau, and J. P. Visticot, Int. Rev. Phys. Chem. **22**, 285 (2003).
[8] W. G. Roeterdink and M. H. M. Janssen, Phys. Chem. Chem. Phys. **4**, 601 (2002).
[9] R. Wester, A. E. Bragg, A. V. Davis, and D. M. Neumark, J. Chem. Phys. **119**, 10032 (2003).
[10] V. Blanchet, M. Z. Zgierski, and A. Stolow, J. Chem. Phys. **114**, 1194 (2001); M. Schmitt, S. Lochbrunner, J. P. Shaffer, J. J. Larsen, M. Z. Zgierski, and A. Stolow, *ibid.* **114**, 1206 (2001).
[11] V. Engel and H. Metiu, J. Chem. Phys. **90**, 6116 (1989); Chem. Phys. Lett. **155**, 77 (1989); C. Jouvet, S. Martrenchard, D. Solgadi *et al.*, J. Phys. Chem. A **101**, 2555 (1997).
[12] S. I Ionov, G. A. Brucker, C. Jaques, Y. Chen, and C. Wittig, J. Chem. Phys. **99**, 3420 (1993).
[13] I. Bezel, P. Ionov, and C. Wittig, J. Chem. Phys. **111**, 9267 (1999); I. Bezel, D. Stolyarov, and C. Wittig, J. Phys. Chem. A **103**, 10268 (1999).
[14] D. Stolyarov, E. Polyakova, I. Bezel, and C. Wittig, Chem. Phys. Lett. **358**, 71 (2002).
[15] B. Abel, B. Kirmse, J. Troe, and D. Schwarzer, J. Chem. Phys. **115**, 6522 (2001).
[16] B. Abel, N. Lange, and J. Troe, J. Chem. Phys. **115**, 6531 (2001).
[17] B. Abel, S. Y. Grebenshchikov, R. Schinke, and D. Schwarzer, Chem. Phys. Lett. **368**, 252 (2003).
[18] R. Jost, J. Nygard, A. Pasinski, and A. Delon, J. Chem. Phys. **105**, 1287 (1996).
[19] B. Kirmse, A. Delon, and R. Jost, J. Chem. Phys. **108**, 6638 (1998); A. Delon and R. Jost, *ibid.* **110**, 4300 (1999); S. Heilliette, A. Delon, P. Dupre, and R. Jost, Phys. Chem. Chem. Phys. **3**, 2268 (2001); A. Delon, R. Jost, and M. Jacon, J. Chem. Phys. **114**, 331 (2001).
[20] D. C. Robie, M. Hunter, J. L. Bates, and H. Reisler, Chem. Phys. Lett. **193**, 413 (1992).
[21] A. Sanov, C. R. Bieler, and H. Reisler, J. Phys. Chem. **99**, 13637 (1995); S. A. Reid, A. Sanov, and H. Reisler, Faraday Discuss. **102**, 129 (1995).
[22] O. L. A. Monti, H. Dickinson, S. R. Mackenzie, and T. P. Softley, J. Chem. Phys. **112**, 3699 (2000).
[23] A. J. C. Varandas, J. Chem. Phys. **119**, 2596 (2003).
[24] J. H. Schryber, O. L. Polyansky, P. Jensen, and J. Tennyson, J. Mol. Spectrosc. **185**, 234 (1997).
[25] V. P. Hradil, T. Suzuki, S. A. Hewitt, P. L. Houston, and B. J. Whitaker, J. Chem. Phys. **99**, 4455 (1993).
[26] A. V. Demyanenko, V. Dribinski, H. Reisler, H. Meyer, and C. X. W. Qian, J. Chem. Phys. **111**, 7383 (1999).
[27] J. A. Davies, J. E. LeClaire, R. E. Continetti, and C. C. Hayden, J. Chem. Phys. **111**, 1 (1999).
[28] J. A. Davies, R. E. Continetti, D. W. Chandler, and C. C. Hayden, Phys. Rev. Lett. **84**, 5983 (2000).

[29] R. P. Singhal, H. S. Kilic, K. W. D. Ledingham, C. Kosmidis, T. McCanny, A. J. Langley, and W. Shaikh, Chem. Phys. Lett. **253**, 81 (1996).
[30] R. B. Lopez-Martens, T. W. Schmidt, and G. Roberts, J. Chem. Phys. **111**, 7183 (1999).
[31] L. Dinu, A. Eppink, F. Rosca-Pruna, H. L. Offerhaus, W. J. van der Zande, and M. J. J. Vrakking, Rev. Sci. Instrum. **73**, 4206 (2002).
[32] A. T. J. B. Eppink and D. H. Parker, Rev. Sci. Instrum. **68**, 3477 (1997).
[33] The angular resolution of the photoelectron images is unaffected in this configuration.
[34] A. T. J. B. Eppink and D. H. Parker, in *Imaging in Molecular Dynamics: Technology and Applications*, edited by B. J. Whitaker (Cambridge University Press, Cambridge, 2003).
[35] A. T. J. B. Eppink, S.-M. Wu, and B. J. Whitaker, in *Imaging in Molecular Dynamics: Technology and Applications*, edited by B. J. Whitaker (Cambridge University Press, Cambridge, 2003), pp. 65.
[36] B. Abel, N. Lange, F. Reiche, and J. Troe, J. Chem. Phys. **110**, 1389 (1999).
[37] B. G. Lindsay, M. A. Mangan, H. C. Straub, and R. F. Stebbings, J. Chem. Phys. **112**, 9404 (2000).
[38] Chemistry WebBook http://webbook.nist.gov (National Institute of Standards and Technology, 2003).
[39] K. S. Haber, J. W. Zwanziger, F. X. Campos, R. T. Wiedmann, and E. R. Grant, Chem. Phys. Lett. **144**, 58 (1988).
[40] G. Hezberg, *Molecular Spectra and Molecular Structure: III. Electronic Spectra and Electronic Structure of Polyatomic Molecules* (Van Nostrand, New York, 1966).
[41] F. Assenmacher, M. Gutmann, F. Noack, V. Stert, and W. Radloff, Appl. Phys. B: Lasers Opt. **B71**, 385 (2000).
[42] P. I. Ionov, I. Bezel, S. I. Ionov, and C. Wittig, Chem. Phys. Lett. **272**, 257 (1997).